CFSRC COLLOQUIUM

Distortion Buckling Test and Design Method of Cold-Formed Thin-Wall Steel Built-Up Members Under Axial Compression
20-22 October 2020 (cfsrc.org)

Yao Xingyou[1], Li Xiao[2], Cheng Guowei[3], Hu Pengwen[4]

Abstract

The objective of this paper is to research the distortion buckling performance and capacity of cold-formed thin-walled steel built-up I-shaped section column. 12 built-up columns connected by self-drilling screws were conducted under the axial compression. The test members includes four different sections and the specimen length is 1000mm. Test results show that the local buckling and distortion buckling occur for all built-up sections. The finite element software ABAQUS was used to analysis the test specimens. The finite element results were in good agreement with the experimental results about the buckling mode and load-carrying capacities. The direct strength method is used to calculate the load-carrying capacities of the specimens. The calculation results show that the direct strength method is unsafe, so the direct strength method to calculate distortional buckling strength is modified on the basis of the test results.

[1] Associate Professor, School of Architecture and Civil Engineering, Jiangxi Province Key Laboratory of Hydraulic and Civil Engineering Infrastructure Security, Nanchang Institute of Technology, yaoxingyoujd@163.com
[2] Postgraduate Student, School of Architecture and Civil Engineering, Nanchang Institute of Technology, 648627672@qq.com
[3] Postgraduate Student, School of Architecture and Civil Engineering, Nanchang Institute of Technology, 2445640693@qq.com
[4] Postgraduate Student, School of Architecture and Civil Engineering, Nanchang Institute of Technology, 1960989396@qq.com

1. Introduction

With the development of cold-formed thin-wall steel, more and more members have been widely used in construction projects because of the advantages such as convenient fabrication and higher strength. However, with the increase of application of cold-formed steel, the structure become more complex and the height of the structure increases gradually. It is difficult to meet the design and practical requirements by using a single basic specimen (C, U-section steel) which is often used in buildings. In order to improve the bearing capacity, the build-up members connected using double basic section with the self-drilling screw are used in the buildings. At present, there are some simple design approaches to predict the load-carrying capacities of built-up members. It is necessary to further study the buckling behaviors and the buckling strength for the build-up back-to-back I-shape section members.

Peters[1] carried out a study on the bearing capacity of the build-up specimens with two legs connected by screws. The results showed that the screw spacing had a great influence on the bearing capacity of specimens under axial compression. When the screw spacing was too large or too small, the bearing capacity of specimens under axial compression was obviously reduced, so the screw spacing should be controlled within a reasonable range. Abbasi[2] used the modified stiffness beam element method to analyze the stability performance of build-up section, and the modified line method considered the arbitrary arrangement of screw positions. The influence of screw arrangement on the increase of bearing capacity and the change of corresponding buckling mode of build-up section were analyzed. The simplified calculation method of screw arrangement and section characteristics was given. The axial compression tests of 32 I-section members were carried out[3]. The results were compared with those calculated by using the North American AISIS 100-2007. The results showed that the results predicted using code were conservative, especially for thick-walled cross-section specimens. The experimental value exceeded the calculated value by nearly 60%. Whittle[4] carried out 153 closed box-section specimens composed of two channel steels subjected axial compression. The test results were compared with the bearing capacity calculated by the North American code AISIS 100-2007. The results showed that the results calculated by the code were satisfactory. 16 build-up axially compressed members with sheathing panel had carried out by David[5], which included the buckling mode, the ultimate bearing capacity, combined action, end condition, and interaction buckling. Build-up specimens showed local and global buckling. At the same time, the basic frame of strength design of the build-up members was given. There are some studies on the buckling modes and strength predicted about build-up I-section steel members, But it is still necessary to study the buckling behaviors and the distortional buckling strength for the build-up back-to-back I-shape section members.

The distortional buckling behavior and calculated method for the cold-formed thin-walled steel build-up I-section members with nominal yield strength 550MPa under axial compression is experimented. The influence of screw spacing and section size on the bearing capacity under axial compression are studied by test and the finite element ABAQUS and a more suitable modified formula about distortional buckling strength based on direct strength method is proposed.

2. Experimental investigation

2.1 Test specimens and labelling

The cold-formed thin-walled steel I-section specimens includes three kinds of cross-sections, which are 75 series (web depth 75 mm), 80 series (web depth 75 mm) and 100 series (web depth 100 mm). which is shown in Figure 1. In the figure, h, b, and a are the web depth, flange width and lip width, t is plate thickness, e is the distance from self-drilling screw to the midline of cross-section. The specimen nominal length is 1000mm, and the screw spacing is divided into 150 mm and 300 mm. ST4.8 self-drilling screw is used for all specimens in this test (Figure 2). The transverse screw spacing is half of the web length and is arranged in the middle. The test specimens were labeled as shown in Figure 3.The cross-sectional dimensions are given in Tables 1 which are the average measured values for each channel of the test specimens in this study.

Table 1: Measured dimensions of the section

Specimen	L（mm）	Specimen number	Cross-sectional dimensions（mm）				
			h/mm	b/mm	a/mm	t/mm	A(mm^2)
DC7510-10-S150-N-1	999.5	a	74.03	39.91	9.59	0.93	321.84
		b	74.14	39.76	10.14	0.93	
DC7510-10-S150-N-2	1000	a	74.93	39.34	10.00	0.93	322.35
		b	74.18	39.84	9.72	0.93	

DC7510-10-S300-N-1	1000	a	73.42	39.33	10.17	0.93	320.70
		b	74.42	40.42	10.25	0.93	
DC7510-10-S300-N-2	999.5	a	73.20	39.89	9.80	0.93	320.99
		b	73.43	39.98	9.30	0.93	
DC10010-10-S150-N-1	999.75	a	97.55	89.78	9.82	0.93	551.21
		b	97.26	89.73	9.81	0.93	
DC10010-10-S150-N-2	999.35	a	97.08	89.71	10.17	0.93	549.96
		b	96.45	90.15	9.47	0.93	
DC10010-10-S300-N-1	1000	a	96.88	90.00	9.81	0.93	551.49
		b	97.19	89.82	9.88	0.93	
DC10010-10-S300-N-2	1000	a	96.65	90.18	9.80	0.93	551.68
		b	97.00	89.95	10.10	0.93	
DC8008-10-S150-N-1	999.75	a	79.38	59.76	9.74	0.73	318.85
		b	79.15	59.14	10.12	0.73	
DC8008-10-S150-N-2	999.6	a	78.11	60.21	9.66	0.73	318.05
		b	79.05	59.79	9.42	0.73	
DC8008-10-S300-N-1	1000	a	79.70	59.93	9.85	0.73	320.12
		b	79.57	59.06	9.90	0.73	
DC8008-10-S300-N-2	1000	a	78.04	59.64	10.00	0.73	317.27
		b	78.90	59.68	9.76	0.73	

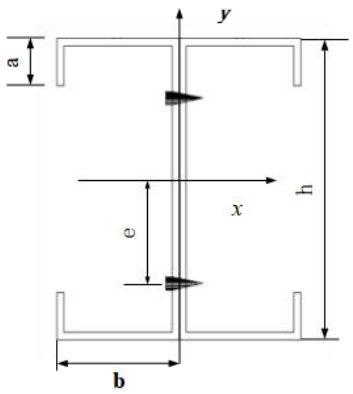

Figure 1: The back-to-back section connected with web screws


Figure 2: Self- drilling screws

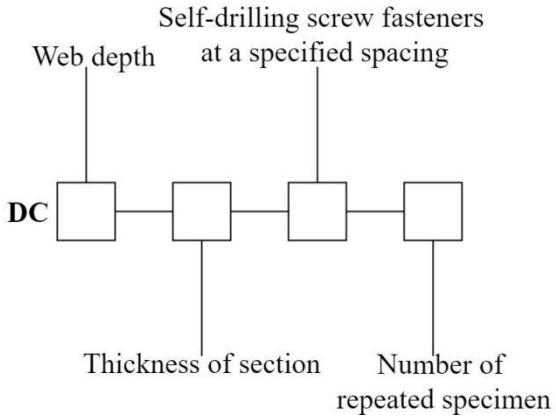

Figure 3: Specimen label

2.2 Material Properties

The test specimens were processed from two kinds of steels with different thicknesses. Tensile coupon tests of flat portions of cross sections were conducted for each thickness to determine the material properties based on Chinese specifications of "Tensile tests of metallic materials-part 1: test methods at room temperature"(GB/T228.1—2010)[6]. The failure characteristics and the stress-strain curves of the coupon test specimens are shown in Figs. 4 and 5, respectively. The measured material properties including the static 0.2% proof stress($\sigma_{0.2}$) and initial Young's modulus (E) are

600Mpa, 216000Mpa and 610Mpa, 216000Mpa for 0.93mm thickness and 0.73mm thickness plates, respectively.

(a) 0.93mm plate thickness (b) 0.73mm plate thickness

Figure 4: Failure characteristics of coupon tests

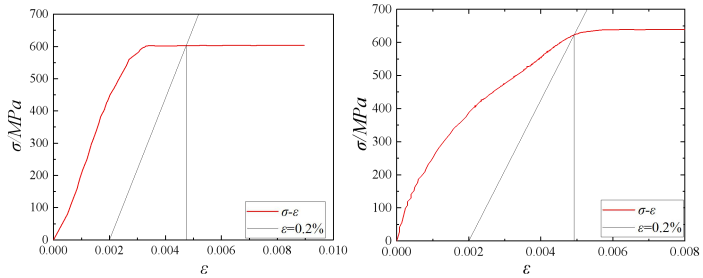

(a) 0.93mm plate thickness (b) 0.73mm plate thickness

Figure 5: Stress-strain curves of coupon tests

2.3 Test setup and procedure

The built-up specimens were loaded by hydraulic universal material testing machine (Figure 6). YJ16 data acquisition instrument was used to automatically collect the test data. The boundary conditions at the ends of all test specimens are hinged support. Both ends of the specimens are equipped with top and bottom knife edge and the size is 300mm×400mm×15mm. In order to understand clearly the displacement and deformation of the specimen during the loading process, six displacement meters are arranged at the mid-length of column, and a displacement meter is arranged at the upper end plate of the specimen to measure the vertical load. The specific arrangement is shown in Figure 7.

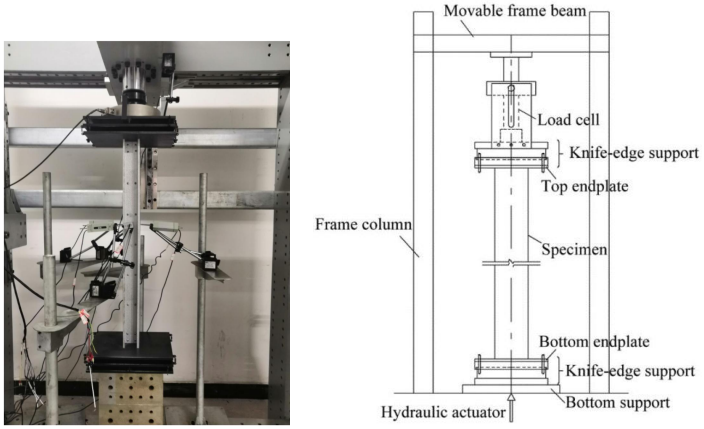

Figure 6: Typical experimental setup of axially-compressed tests of built-up open sections

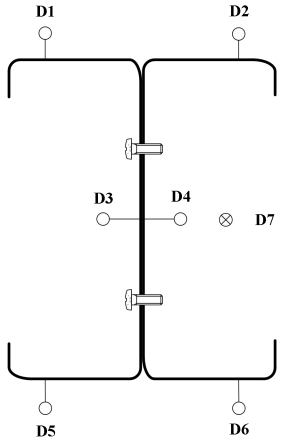

Figure 7: Arranged displacement transducers

2.4 Test results

2.4.1 Buckling behavior

For the DC10010 and DC8008 sections which has a relatively large width-thickness ratio of flange, the local buckling appears at the web with the increase of load. Then the distortional buckling occurs when the load continues to increase. when the load continues to increase, the specimen's distortional buckling deformation increases, which shows that the distortional buckling has high post-buckling strength. The final failure modes of the specimen are interaction of local buckling and distortion buckling, as shown in Figure 8(a)-(b).

(a) DC10010-S150-N

(b) DC8008-S150-N

Figure 8: Distortional buckling failure modes of DC10010-S150-N and DC8008-S150-N

For the DC7510 sections which has a relatively small width-thickness ratio of flange, the local buckling appears at the web with the increase of load(Figure 9(a)). Then the slight distortional buckling deformation occurs when the load continues to increase. when the load continues to increase, the specimen's distortional buckling deformation increases and the end of specimen are crushing. The final failure modes of the specimen are interaction of local buckling and distortion buckling, as shown in Figure 9(b).

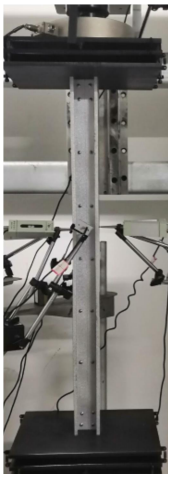

(a) Local

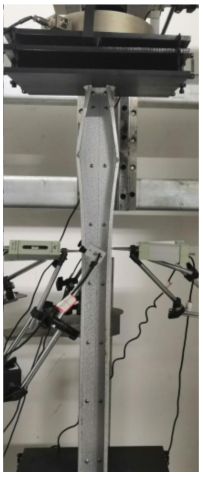

(b) Distortional buckling

Figure 9: Failure modes of DC7510-S150

With the changing of the self-drilling screw spacing from 150mm to 300mm, the buckling mode have no change. The self-drilling screw can make the two lipped channel section work together. The buckling modes are shown in Figure 10.

(a) DC10010-S150-N

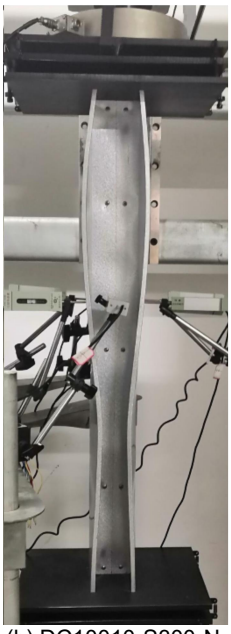

(b) DC10010-S300-N

Figure 10: Influence of specified spacing

2.4.2 Load-displacement curves

The load-displacement curves for all the specimens are shown in Figure 11. As shown in Figure 11, the peak values of specimens with the 150mm and 300mm screw spacing are relatively close and the differences are within 5%. The comparisons indicate that the changing of the screw spacing has a relatively small effect on the ultimate bearing capacity of the specimen. for the same section specimens, the reduce of the screw spacing has a certain effect on the rigidity of the specimens.

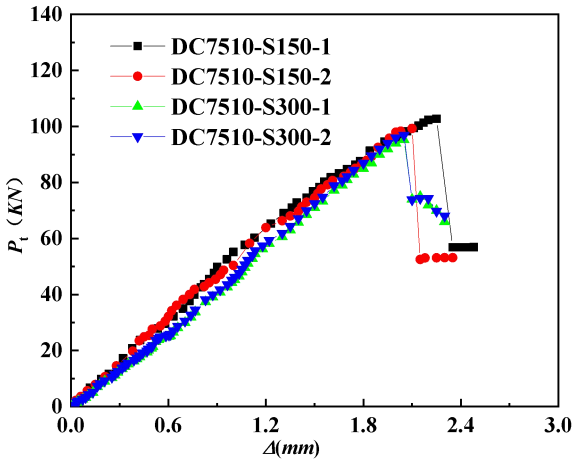

(a) DC7510

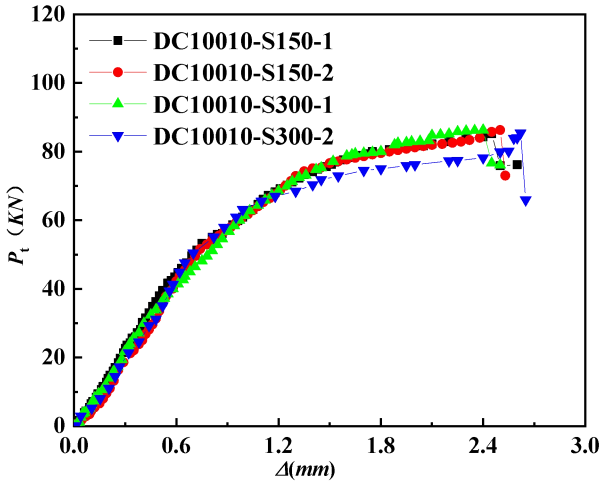

(b) DC10010

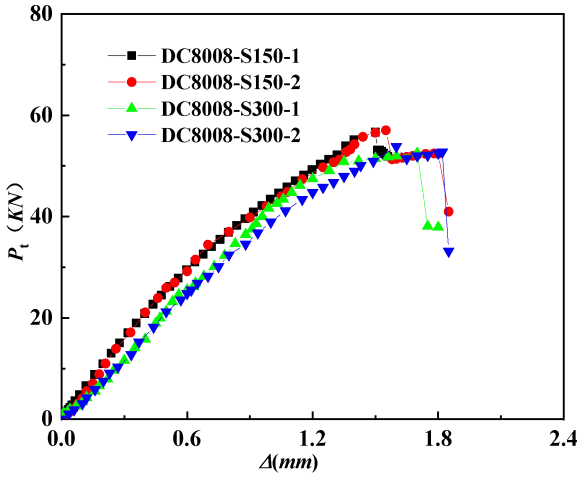

(c) DC8008

Figure 11: Load-axial displacement curves

2.4.3 Load-bearing capacity analysis

In the North American "Specification for the design of cold-formed steel structural members"(AISI S100-2016)[7] , the direct strength method (DSM) adopts the full section to calculate the bearing capacity of members, and the local buckling and distortional buckling of members are considered. The ultimate strength of axially-compressed members is $Pn = min\{Pnl, Pnd\}$, where Pnl、Pnd are predicted using the following formulas:

$$\text{when}\lambda_l \le 0.776, P_{nl} = P_{ne} \quad (1)$$

$$\text{when}\lambda_l > 0.776, P_{nl} = \left(1 - 0.15\left(\frac{P_{crl}}{P_{ne}}\right)^{0.4}\right)\left(\frac{P_{crl}}{P_{ne}}\right)^{0.4} P_{ne} \quad (2)$$

$$\text{when}\lambda_d \le 0.561, \ P_{nd} = P_y \quad (3)$$

$$\text{when}\lambda_d > 0.561, Pnd = \left(1 - 0.25\left(\frac{P_{crd}}{P_y}\right)^{0.6}\right)\left(\frac{P_{crd}}{P_y}\right)^{0.6} P_y \quad (4)$$

when: $\lambda_l = \sqrt{P_{ne}/P_{crl}}$, $\lambda_d = \sqrt{P_y/P_{crd}}$,$P_{ne}$,$P_{nl}$ and P_{nd} are the critical elastic overall, local, and distortional buckling capacities, which can be calculated by CUFSM using the built-up sections.

The ultimate bearing capacity predicted by using direct strength method(P_{DSM}) and tests results(P_t) are shown in Table 2. it can be seen from Table 2, the calculation results by using direct strength method are unsafe, which is 20% to 50% larger than the test value.

Table 2: Comparison on ultimate strengths and buckling modes obtained from test, FEA results, DSM predictions and modified DSM predictions subjected to distortional buckling

Specimens	Tests		FEA		DSM	Modified DSM	Comparison		
	P_t	Failure mode	PFEA	Failure mode	PDSM	PMDSM	PFEA $/P_t$	PDSM $/P_t$	PMDSM $/P_t$
DC7510-10-S150-N-1	102.7	L+D	105.80	L+D	126.31	90.52	1.03	1.23	0.88
DC7510-10-S150-N-2	99.35	L+D	103.00	L+D	126.15	90.36	1.04	1.27	0.91
DC7510-10-S300-N-1	95.3	L+D	101.30	L+D	122.68	87.60	1.06	1.29	0.92
DC7510-10-S300-N-2	96.86	L+D	102.00	L+D	123.33	88.13	1.05	1.27	0.91
DC10010-10-S150-N-1	85.23	L+D	83.47	L+D	105.51	73.76	0.98	1.24	0.87
DC10010-10-S150-N-2	86.28	L+D	84.31	L+D	105.54	73.78	0.98	1.22	0.86
DC10010-10-S300-N-1	86.29	L+D	83.45	L+D	105.42	73.70	0.97	1.22	0.85
DC10010-10-S300-N-2	85.36	L+D	84.29	L+D	105.46	73.72	0.99	1.24	0.86
DC8008-10-S150-N-1	56.58	L+D	54.32	L+D	79.55	56.99	0.96	1.41	1.01
DC8008-10-S150-N-2	57.04	L+D	55.40	L+D	79.35	56.82	0.97	1.39	1.00
DC8008-10-S300-N-1	52.53	L+D	53.35	L+D	79.87	53.25	1.02	1.52	1.01
DC8008-10-S300-N-2	53.84	L+D	53.88	L+D	79.16	53.69	1	1.47	1.00
Mean	—	—	—	—	—	—	1.004	1.314	0.923
SD	—	—	—	—	—	—	0.034	0.105	0.064
COV	—	—	—	—	—	—	0.034	0.080	0.069

Note: L = local buckling; D = distortional buckling.

3. Finite element simulation

3.1 Development of finite element models

The S4R shell element is selected for modelling column and the analytical rigid body element is used for the upper and lower end plates of the specimen. The ST4.8 self-drilling screw is used in this experiment. In order to ensure the accuracy of the finite element, the C3D8R solid element is used to simulate the self-drilling screw. The self-drilling screw and the web are connected by Tie (binding). Because the two web surfaces are prone to puncture in the finite element method, the hard contact between the contact surfaces of the components can only transfer the normal stress between the two surfaces. The surface of the component is relatively smooth, the influence of friction is small, and "no friction" is set in the finite element method. The end constraint conditions of the test plate are all hinged, by constraining the four degrees of freedom of the upper end plate reference point RP1 (2 translation degrees of freedom and 1 rotational degree of freedom, releasing

UZ degrees of freedom to control displacement) and the lower end plate center reference point RP23 translation degrees of freedom and Z-direction rotational degrees of freedom. The final finite element model is shown in Figure 12.

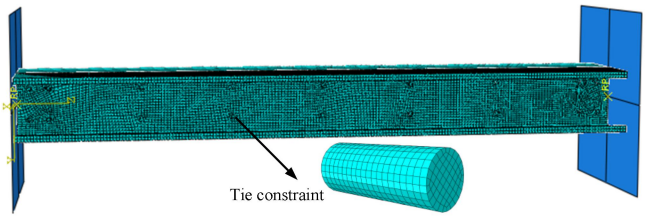

Figure 12: Finite element model

3.2 Verification of finite element models

The experimental and numerical results are compared in Table 2. The mean value of the finite element analysis(FEA) to experimental capacity (P_{FEA}/P_t) ratio is 1.004 with the coefficient of variation (COV) of 0.034. The failure modes of the built-up section columns obtained from FEA at ultimate load were also compared with the tests as shown in Figs. 13, the local buckling and distortional buckling failure can be seen. The comparisons show very good agreement between the test and numerical results, which indicates that the finite element models were capable of replicating the buckling behavior of the test built-up specimens. The load-displacement curves for Specimens obtained from the test and FEA are shown in Figure 14. The load-displacement curves predicted by the FEA matches well with the test result. Therefore, the finite element models were verified against the tests and proved to be accurate in terms of ultimate moment, failure mode, and load-displacement curve.

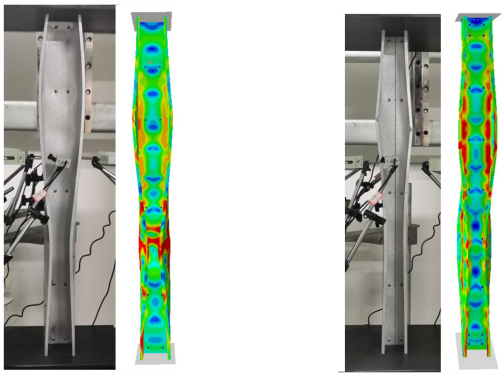

(a) DC10010-S300-N (b) DC8008-S300-N

Figure 13: Comparison between finite element and experimental model

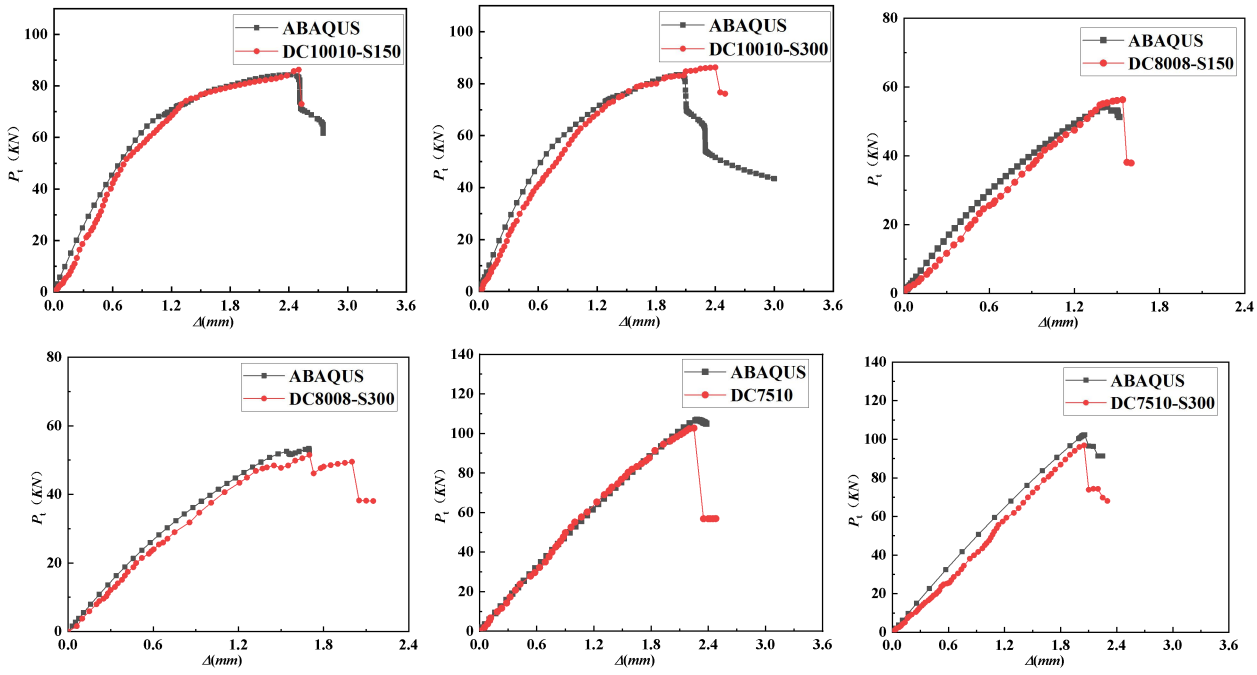

Figure 14: Load-displacement curves between test and finite element

4. Design approaches

Because the distortional buckling mainly occurs in the selected members, the bearing capacity is controlled by the distortional buckling strength, the solution of P_{nd} is modified. The modified distortion buckling formula is:

$$\lambda_d \leq 0.353, P_{nd} = P_y \quad (5)$$

$$0.353 < \lambda_d < 0.786, P_{nd} = (1.216 - 0.612(\frac{P_y}{P_{crd}})^{0.5})P_y \quad (6)$$

$$\lambda_d \geq 0.786, P_{nd} = \left[1 - 0.34(\frac{P_{crd}}{P_y})^{0.8}\right](\frac{P_{crd}}{P_y})^{0.8}P_y \quad (7)$$

The calculated results using The modified distortion buckling formula are shown in Table 2. The average value of ratio of the modified value P_{MDSM} to the experimental value P_t is 0.923, and the coefficient of variation is 0.069.the modified distortional buckling design curve, code design curve, and test resluts are shown in Figure 15. the modified distortional buckling design curve is more consistent with test results. These results shown that the modified distortional buckling design curve can accurate predict the load-carrying capacities of cold-formed thin-walled steel built-up I-shaped section column.

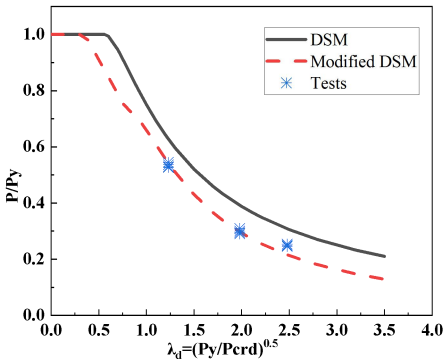

Figure 15: Comparison of design strengths with test and distortional buckling design curve

5. Conclusions

Test results show that the local buckling and distortion buckling occur for all built-up sections. The finite element software ABAQUS was used to analysis the test specimens. The finite element results were in good agreement with the experimental results about the buckling mode and load-carrying capacities. The direct strength method is used to calculate the load-carrying capacities of the specimens. The calculation results show that the direct strength method is unsafe, so the direct strength method to calculate distortional buckling strength is modified on the basis of the test results.

The distortion buckling performance and capacity of cold-formed thin-walled steel built-up I-shaped section column under axial compression are studied in this paper, the following conclusions are drawn. 1)The 12 built-up member test shows that the local buckling and distortion buckling occur for all built-up sections. the section dimension of the build-up specimen has a great influence on ultimate strength. The bearing capacity will decrease with the increase of the width-thickness ratio of the flange. The self-drilling screw spacing have litter effect on ultimate strength when the spacing changes from 150mm to 300mm. 2)The test members are analyzed and simulated by ABAQUS. the finite element models are verified against the tests and proved to be accurate in terms of ultimate moment, failure mode, and load-displacement curve. 3)Based on the test results, the modified direct strength method for predicting distortional buckling strength is accurate.

6. Acknowledgments

The author gratefully acknowledgements the financial support provided by *National Natural Science Foundation Projects of China(No:51868049)*, *Department of Education Science and Technology Projects of Jiangxi Province in China (No:GJJ180932, GJJ170983)*,*Natural Science Foundation Projects of Jiangxi Province in China (No:20181BAB206040)*,*Nanchang Institute of Technology 2019 Postgraduate Innovation Program (No:YJSCX20190012)* and *Academic and Technical Leaders in Major Subject Areas projects of Jiangxi Province in China(No: 20172BCB22022)*.

References

[1] Peters G K. An investigation of the effects of fastener spacing in built-up cold-formed steel compression members.Halifax: University of Dalhousie,2003.

[2] Abbasi M, Khezri M, Rasmussen K.J.R, Schafer B.W. Elastic buckling analysis of cold-formed steel built-up sections with discrete fasteners using the compound strip method. Thin-Walled Structures, 2018, 124:58-71.

[3] Stone T. A., Laboube R A . Behavior of cold-formed steel built-up I-sections[J]. Thin-Walled Structures, 2005, 43(12):1805-1817.

[4] Whittle J,Ramseyer C.Buckling capacities of axially loaded, cold-formed, built-up C-channels.Thin-Walled Structures,2009,47(2):190-201.

[5] David C. F, Shahabeddin T, Xi Z. et al. Experimental study on the build-up action in sheathed and bare built-up cold-formed steel specimens. Thin-Walled Structures, 2018, 127:290-305.

[6] GB/T 228.1-2010 Test method for tensile test room temperature of metallic materials [S].BeiJing: China Standard Publishing House, 2011.

[7] AISI S100-16, North American Specification for the Design of Cold-Formed Steel Structural Members. Washington, DC, U.S.A.: AISI, 2016.